

*Clinical Investigation***Thermal Decomposition of Human Tooth Enamel**

D.W. Holcomb and R.A. Young

EES and School of Physics Georgia Institute of Technology, Atlanta, Georgia 30332, USA

Summary. Further insight into human tooth enamel, dense fraction (TE), has been obtained by following the change and loss of CO_3^{2-} , OH^- , structurally incorporated H_2O , Cl^- , and, indirectly, HPO_4^{2-} after TE had been heated in N_2 or vacuum in the range 25–1000°C. Quantitative infrared spectroscopic, lattice parameter, and thermogravimetric measures were used. Loss of the CO_3^{2-} components begins at much lower temperature (e.g., 100°C) than previously recognized, which has implications for treatments in vitro and possibly in vivo. CO_3^{2-} in B sites is lost continuously from the outset; the amount in A sites first decreases and then increases above 200° to a maximum at ~800°C (> 10% of the possible A sites filled), where it is responsible for an increase in *a* lattice parameter. A substantial fraction of the CO_3^{2-} in B sites moves to A sites before being evolved, apparently via a CO_2 intermediary. This implies an interconnectedness of the A and B sites which may be significant in vivo. No loss of Cl^- was observed at temperatures below 700–800°C. Structural OH^- content increases ~70% to a maximum near 400°C. Structurally incorporated water is lost continuously up to ~800°C with a sharp loss at 250–300°C. The “sudden” *a* lattice parameter contraction, ~0.014Å, occurs at a kinetics-dependent temperature in the 250–300°C range and is accompanied by reordering and the “sharp” loss of ~1/3 of the structurally incorporated H_2O . The hypothesis that structurally incorporated H_2O is the principal cause of the enlargement of the *a* lattice parameter of TE compared to hydroxyapatite (9.44 vs 9.42Å) is thus allowed by these experimental results.

Key words: Tooth enamel — Thermal decomposition — Water — CO_3 — Hydroxyl.

Introduction

There is much yet to be learned about how the component parts of human tooth enamel combine to make it what it is. One approach is to study how the components disassemble, change, and are lost as tooth enamel, in this case the dense fraction (TE), is heated to successively higher temperatures. Components particularly subject to such study, up to ~1000°C, are H_2O , $(\text{HPO}_4)^{2-}$, $(\text{OH})^-$, $(\text{CO}_3)^{2-}$, and Cl^- . Reported amounts present in TE are 5–6 wt% for H_2O (e.g. [1]) ~3 wt% CO_3 [2] and ~5 wt% HPO_4 [3].

There have been several previous studies on pyrolysis of TE that are closely related to the present work. In a series of papers, LeGeros and co-workers [4–6], igniting TE first at 200° and later at 100°C increments, used X-ray diffraction, thermogravimetric analysis (TGA), and infrared spectroscopy (i.r.) to study several features and, *inter alia*, concluded that “lattice H_2O ” is responsible for the *a* axis of untreated TE being ~0.02 Å larger than it is in hydroxyapatite and larger than it is in TE that has been heated to 400°C. They have also noted that heating to 600°C, and even more so to 800°C, increases the room temperature *a* lattice parameter. These observations are corroborated and explained in the present work.

Corcia and Moody [7] did a combined TGA study and mass spectrometry of the evolved species in the pyrolysis of TE. Little and Casciani [1] and Myrberg [8] used TGA and nuclear magnetic resonance (NMR) analysis of specimens “pyrolyzed” at various temperatures to pursue Myers’ [9] suggestion of entrapped water in TE. They are in general agreement that a substantial fraction of the 5–6 wt% water in TE is somehow “caged” or zeolitic. Holager [10] did comparative TGA on TE and dentine. Brauer, Termini, and Burns [11] include a differential thermal analysis curve for TE.

Send offprint requests to R.A. Young at the above address.

It was established by Elliott [2] with polarized i.r. that CO_3^{2-} in TE occurs in two different environments. Emerson and Fischer [12] had noted that on heating TE to 800°C there were changes in the relative intensities among some of the i.r. carbonate bands, those now identified with A-site CO_3^{2-} (e.g., 883, 1465, and 1542 cm^{-1} cited by Bonel and Montel [13]; 879, 1465, and 1546 cm^{-1} found here) increasing and those identified with the initially dominant B sites (864 , 1430 , and 1455 cm^{-1} cited [13]; 872 , 1415 , and 1455 cm^{-1} found here) decreasing. Thus possible migration was implied, and may have been suspected [14, 15], of CO_3^{2-} from B sites, containing $\sim 85\%$ of the CO_3^{2-} in untreated TE and associated with PO_4^{3-} positions [2, 13, 16], to A sites associated with hydroxyl ion positions [2, 13] when TE was heated to 800°C . Therman and Elliott [15] have further studied the thermally produced changes in the i.r. spectra of CO_3^{2-} in carbonate-containing apatites and TE. They again observed that the decrease in B-type CO_3^{2-} was accompanied by an increase in A-type CO_3^{2-} up to temperatures $> 800^\circ\text{C}$, whereafter A-type also decreased. Further, they observed a CO_2 band at 2340 cm^{-1} . (They also observed a 2010 cm^{-1} band in synthetic CO_3^{2-} -containing apatites but not in TE, and 2200 cm^{-1} in TE but not in synthetics prepared in the absence of NH_3 .) With polarized i.r. and isotopic shifts they showed that the moiety giving rise to the 2200 cm^{-1} band was N-C-O and was oriented with the N-C-O direction along the apatite crystallographic c axis. The CO_2 associated with the 2340 cm^{-1} band was in random orientation. They also noted an increase in the OH-stretch (3569 cm^{-1}) band intensity and a decrease in the H_2O band with heating, as have other workers, e.g. [17]. LeGeros, Bonel, and Legros [6] noted a change in the OH-stretch band but described it as sharpening, which also occurs, rather than increase.

Arends and Davidson [3] reported a method for distinguishing the HPO_4^{2-} contribution from overlapping CO_3^{2-} contributions in the i.r. spectra. Davidson and Arends [18] then used the method to make a TGA, i.r., and X-ray lattice parameter study focusing on HPO_4^{2-} and H_2O in sound and carious TE. They reported $\sim 5\text{ wt}\%$ HPO_4^{2-} in sound human TE.

The present work extends the temperature-scale detail and the quantitation of many of the i.r. results. It increases the range of components simultaneously followed quantitatively (OH^- , H_2O , Cl^- , B- CO_3^{2-} , A- CO_3^{2-} , CO_2 , and HPO_4^{2-}) in the specimens along with TGA, a lattice parameter data, and some i.r. measures of the evolved gases. In so doing, this work corroborates many of the previous results, contradicts others, and produces a number

of new results which add up to an internally consistent picture of the thermal decomposition process.

Materials and Methods

The TE was taken from a pool of the dense fraction (sp.g. > 2.95) of human tooth enamel harvested from several hundred teeth extracted in the Atlanta area. Carious portions were excised, the pellicle was burnished off with a dental hand-piece, and the dentin was ground away from the inside. These enamel caps were then crushed to fractional millimeter size and density-separated by flotation in tetrabromoethane. The dense fraction was washed and air dried. Any pieces that fluoresced under u.v. light (indicating clinging bits of dentin) were discarded. The remainder was stored in air until use, at which time it was ground to $< 37\text{ }\mu\text{m}$ (-325 mesh sieve) particle size.

Heating was done in a tube furnace in a slowly flowing N_2 atmosphere under slight positive pressure. Time at temperature was approximately 24 h. For the runs in which H_2O in the specimen was to be determined from the i.r. spectra, the N_2 was specially dried by being passed through $\sim 80\text{ cm}$ of P_2O_5 between the N_2 tank and the furnace. All specimens were cooled to room temperature before they were removed from the N_2 atmosphere and stored in a desiccator over P_2O_5 . Those prepared for the H_2O measurements were kept in the closed desiccator until after it had been transferred to the dry box (N_2), wherein they were made into i.r. specimens in Fluorolube (trifluorovinyl chloride polymers, Hooker Chemical Co.) mulls. The others were pressed in KBr pellets (13 mm diameter discs) in vacuo while warm ($\sim 50^\circ\text{C}$). The specimen compartment of the i.r. unit was continuously purged with dry air (-55°C dew point). The same initial particle size ($< 37\text{ }\mu\text{m}$, determined by 325 mesh sieve) was used for all quantitative i.r. work. After being heat treated, the i.r. specimens were ground in the supporting matrix (KBr or Fluorolube).

The i.r. unit was a Perkin-Elmer 580B (double beam) unit operated with 1.8 cm^{-1} programmed resolution and a full-spectrum scanning time of either 1 or 4 h. The instrument was operated in the linear absorbance mode so that quantitative analyses could be made with the areas under the peaks ('bands'). Pellet loadings were arranged to keep the absorbance, for the bands of interest, in the range 0.2–0.7 except when a moiety was nearly absent. The absorbance of the various moieties was found to be linear up to KBr pellet loadings of $4\text{ mg}/13\text{ mm}$ disc. By repeating KBr pellet preparations and i.r. scans, it was shown that the precision, in determining amount of a component present from the area of one of its i.r. bands, was 10% or better.

Since products of the same heating runs were used for KBr pellets and Fluorolube mulls, the i.r. spectra with the mulls (in which the loading could not be precisely controlled) were scaled to the i.r. spectra with KBr pellets on the basis of the OH-stretch peaks (3569 cm^{-1}).

Typical i.r. spectra are shown in Figure 1a. Band intensities in the i.r. spectra were measured as peak-height-above-background times width-at-half-height. The backgrounds were drawn in as shown, for example, for the CO_3^{2-} bands in Figure 1b. The width was taken to be the width at half height of a triangular approximation to the band profile based on its best resolved portion (Fig. 1b).

In studying the i.r. results presented in this paper, the reader is cautioned to keep in mind that (a) the plots do not directly represent the amount present of a moiety relative to others but represent only the amount relative to itself at the various temper-

TOOTH ENAMEL I.R. SPECTRA
POWDER SAMPLES

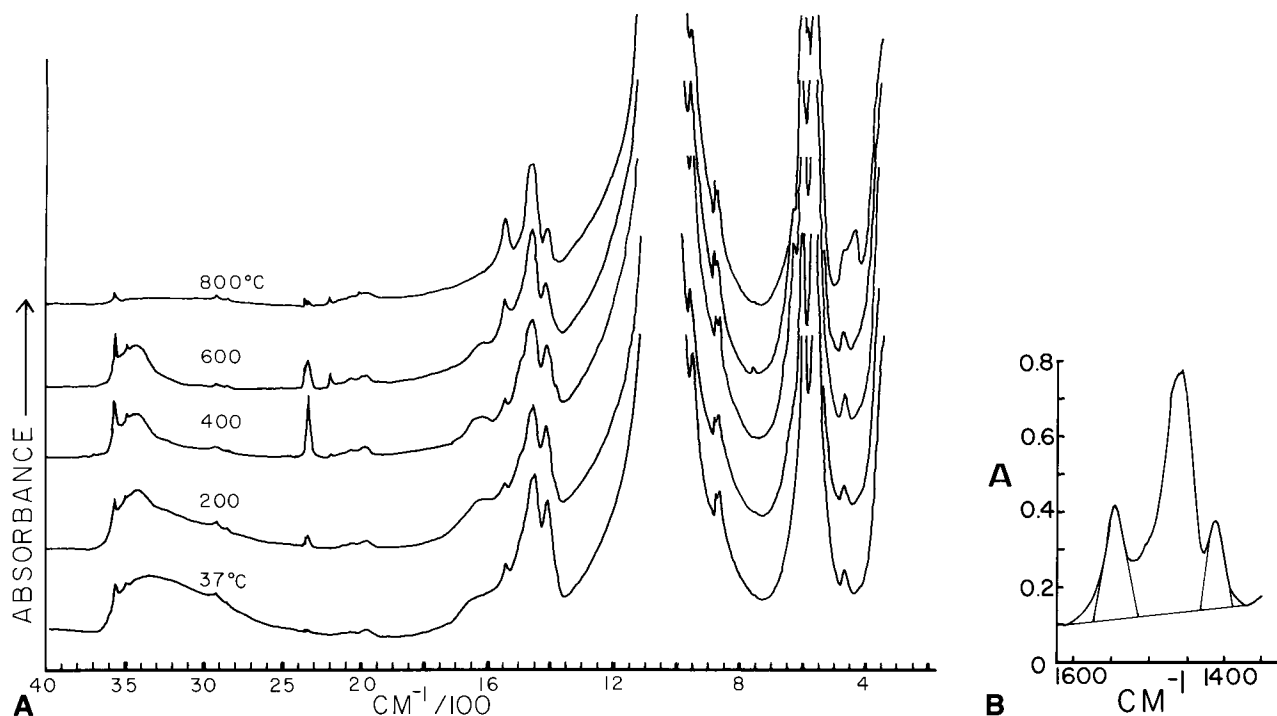


Fig. 1. Infrared spectra of tooth enamel. **A** Typical spectra of TE after being heated to various temperatures. The KBr pellet loadings were deliberately made so high that the phosphate modes ($500\text{--}650\text{ cm}^{-1}$ and $900\text{--}1200\text{ cm}^{-1}$) are off scale in order that the spectral components of interest could be more easily studied. **B** Enlargement (scale expansion) of the CO_3^{2-} bands at 1415 cm^{-1} and 1546 cm^{-1} showing how the background was placed and the areas were estimated

atures; (b) all i.r. specimens were ground to the same particle size before being incorporated in a pellet or mull, but no other correction was made for the heating effect on particle size (any residual effect would be to reduce the observed band intensities at the higher temperatures by a few percent); (c) the i.r. data either are based directly on or are scaled to the same pellet loading with no correction being made for the temperature-induced weight loss. (Thus, for example, the high temperature specimens had a few percent more PO_4^{3-} groups in the i.r. beam than did the low temperature ones.)

For i.r. observation of the evolved gases, a special closed heating cell was built which contained the specimen and fit into the i.r. unit so that the i.r. beam passed longitudinally through the cell. It was basically a silica tube 15 mm in diameter and 80 mm long. After the specimen was placed inside, the ends were closed with CaF_2 windows seated on silicone O-rings and the chamber was then closed off at room temperature. The i.r. spectra were not collected until the specimen temperature had been maintained at the stated value for 24 h.

A heating tape was wrapped several times around the cylinder. Gradients were expected to be large, as the heating tape subtended only about 2π steradians at the specimen. Chamber temperature was monitored with an externally mounted thermocouple. Calibration runs were made with a thermocouple placed in the specimens. Typical differences were 40° at 500°C and 18° at 200°C . The chamber was emptied of the evolved gases between runs at different temperatures. Since the windows were at tem-

peratures below 100°C , evolved H_2O could condense out on them. Therefore the data obtained with this cell are indicative but may not be quantitatively reliable for evolved H_2O .

The TGA unit was operated at $8^\circ\text{C}/\text{min}$ (continuous) with the specimen in vacuum (roughing pump).

The lattice parameter data were obtained in two ways. In one, they were an incidental result of an extensive study of the crystal structure of TE as a function of temperature (P.E. Mackie, personal communication) up to 500°C . The X-ray measurements were made at temperature in vacuo. The time at each temperature was several days, and the specimen was not cooled before being advanced through the next temperature increment. At each temperature, a full powder diffraction pattern was collected in digitized form. Crystal structure refinements with the Rietveld pattern-fitting-structure-refinement method [19] then provided a and c lattice parameter values, among many other results. The values obtained for a during the rising temperature part of the first temperature cycle were corrected to equivalent room temperature a values with the use of the thermal coefficient of expansion, α , found in the decreasing temperature part of the first cycle and both parts of the second ($\alpha(a) = 1.02\text{ \AA}/^\circ\text{C}$). Standard deviations in the determination of a at-temperature were $\sim 0.002\text{ \AA}$.

In the second method, the specimens were heated in a tube furnace for 12–16 h and then cooled to room temperature, all in dried N_2 . A standard X-ray powder diffractometer and $\text{CuK}\alpha$ radiation were used to scan the diffraction pattern from $25^\circ(2\theta)$ to

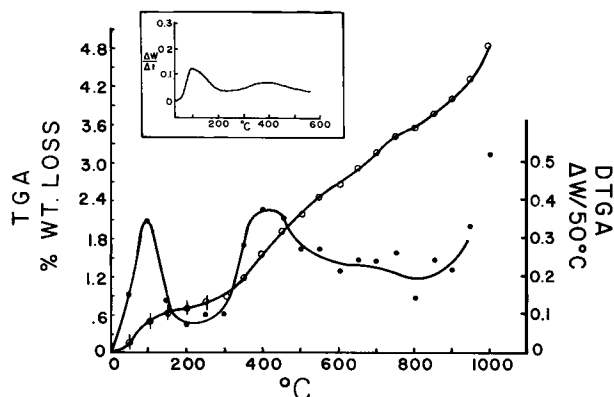


Fig. 2. Weight loss of TE heated at 8°C/min in vacuum. ○ Total weight loss as recorded (TGA = thermogravimetric analysis). ● Temperature derivative of recorded curve (DTGA = difference TGA), as approximated in 50° increments. The inset figure is adapted from Davidson and Arends [18] for sound TE, by scale inversion for easy comparison here

35°(2θ) and positions of 3.00 and 2.10 reflection were read from the strip chart recording. The probable error with this method is estimated to be ~0.005 Å in precision and 2 or 3 times that in accuracy.

Results and Discussion

TGA

The TGA curves obtained for TE (Fig. 2) are much like those obtained by others for similar specimens [e.g., 6, 7, 10, 18, 20].

Although the amounts of weight loss observed vary with reporter and specimen, all of the TGA curves show an initial weight loss, a reduction in slope around 100–110°C, and an increase of slope between 300 and 350°C. Thereafter the slope decreases very gradually up to ~900°C. LeGeros, Bonel, and Legros [6] have reported that, up to 400°C at least, the weight losses at given nominal temperatures were comparable whether measured with the "continuous pyrolysis" TGA method or with a "discontinuous pyrolysis" method in which the sample was heated 5 h at the set temperature, then cooled and weighed at room temperature. The differences they did observe may have been due to atmosphere, not kinetics. (They observed less weight loss in the discontinuous method, which is to be expected because of H₂O adsorption if the specimens were cooled in air.)

Since our "discontinuous pyrolysis" specimens were cooled in N₂, we can expect less difference

than LeGeros et al. [6] observed from the TGA weight loss results because of adsorbed H₂O. On the other hand, our results for H₂O loss and lattice parameter change in N₂ and in vacuum do suggest that the apparent temperature at which weight loss is recorded by TGA is higher than that at which it actually occurs and that heating a long time in vacuum produces equivalent losses of H₂O at still lower temperatures. Accurate identification of correlations, or lack of them, among the different types of measurements is crucial to affirmation or negation of hypothesized cause and effect relationships.

Evolved Gases

Figure 3a shows i.r. spectra of the gases evolved, less any condensation on the chamber walls, in 24 h at various specimen temperatures. Partly because of the condensation, these evolved gases spectra are suitable for qualitative comparison but not for quantitative work such as was possible with the i.r. spectra of the TE specimens. The principal evolved species identified are H₂O vapor (best seen in other spectra, not shown, based on larger samples), CO₂, and unspecified organic gases. (H₂O vapor was characterized by a series of small peaks in the range 3400–3800 cm⁻¹.) We note that CO₂ evolution is started at 180° and is strong at 360° and 460°C. Figure 3b shows in histogram form the CO₂ evolved in each temperature interval.

H₂O

The amount of H₂O measured by i.r. in the TE specimen after heating depended on the atmosphere in which the specimen was heated and cooled and its subsequent exposure to air. Figure 4 shows the results for TE maintained in a specially dried N₂ atmosphere throughout heating, cooling, and mulling in Fluorolube. The parameter plotted is the height of the i.r. curve at 3300 cm⁻¹ above a background taken from the i.r. "spectrum" in that region for TE heated at 1000°C (Fig. 1). The choice of 3300 cm⁻¹ was based on the following. In another work with KBr pellets it was noted that the "broad water" hump from 2300 to 3600 cm⁻¹ seemed to be composed of two humps, one peaking near 3430 cm⁻¹ and one near 3300 cm⁻¹. By noting which one moved with deuteration and which one changed with degree of exposure to the atmosphere (Fig. 5a), we determined that the one centered at 3430 cm⁻¹ was due to adsorbed, and possibly sorbed,

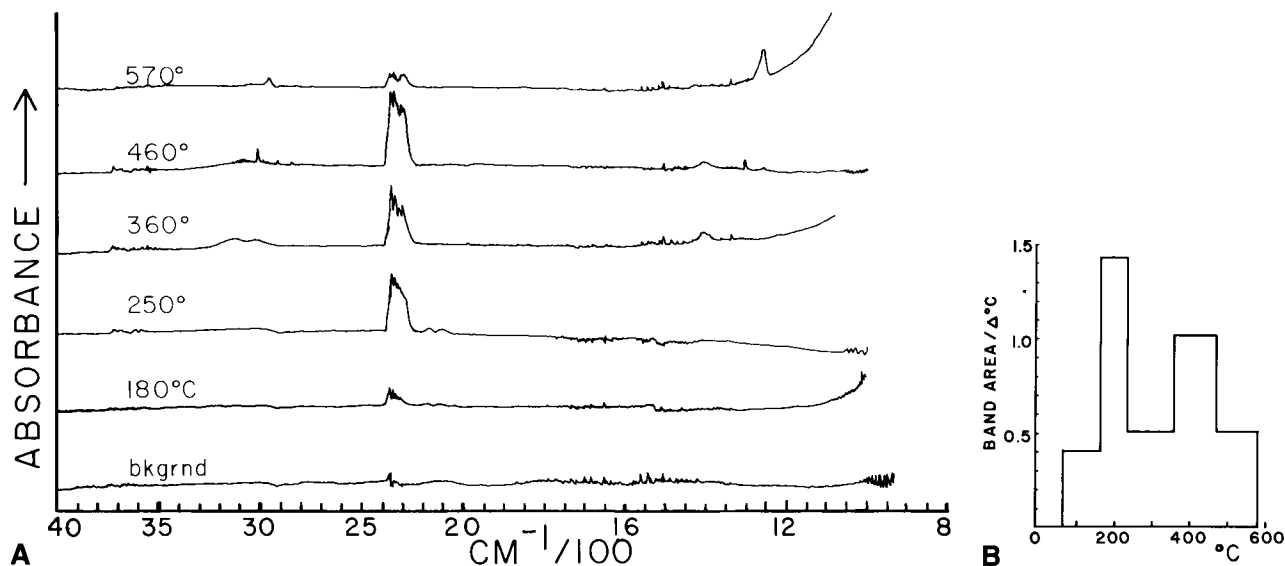


Fig. 3. A Gases evolved from TE. i.r. spectra of gases, collected in cell, evolved between indicated temperature and next lower one. Cell was held 24 h at indicated temperature. Some possible band assignments are listed below.¹ B CO₂ evolved between temperatures, as determined from area of the ~2340 cm⁻¹ band in i.r. spectra of the evolved gases. The area in each segment corresponds to the band area

H₂O, while the 3300 cm⁻¹ one seemed to be more intimately a part of TE itself. We shall refer to the latter as "incorporated H₂O." The actual partition of the "broad water hump" into the two could be done only approximately. Figure 5b shows a visual estimate. Note that, at least in this estimate, the hump centered at about 3430 cm⁻¹ contributes little to the height of the total curve above background at 3300 cm⁻¹.

The i.r. specimen preparation procedure used for these retained H₂O measurements was intended to exclude entirely the type of H₂O giving rise to the broad band centered near 3430 cm⁻¹. However, these procedures probably could not be fully effective on specimens that had never been heated much above 100°C to remove the adsorbed and sorbed water in the first place. Thus the 25°C and 110°C points in Figure 4 may be artificially high, by some unknown small amount (a few percent) be-

cause of contribution from a 3430 cm⁻¹ broad band. Nonetheless, in Figure 4 it is clear that a rather dramatic loss of incorporated H₂O, nearly one-third of the amount initially present, occurs between 270° and 300°C. But a small fraction of the incorporated H₂O seems to be retained—or resupplied by decomposition of other components—even up to 800°C.

Hydroxyl and Chloride Ions

It has been noted by several workers, for example, by R.Z. LeGeros (personal communication, 1972) and [15, 17, 21], that the OH-stretch band at 3569 cm⁻¹ increases when TE is heated. This band occurs 1 or 2 wavenumbers higher in hydroxyapatite. The present measurements (Fig. 6) of the area of the 3569 cm⁻¹ i.r. peak show that between room temperature and 400°C there is a large increase, ~70%, in the number of "structural OH" ions, i.e., in their normal hydroxyapatite (OHAp) sites. In the section on CO₃²⁻, we show that the CO₃²⁻ breakdown by reaction with H₂O—presumably present near the A-CO₃²⁻ site—is probably the source of only a small part of these "new" OHs by CO₃²⁻ + H₂O → CO₂ + 2(OH)⁻. At the same time that it is increasing, the 3569 cm⁻¹ band does narrow by about 30%, showing that the ordering of the OHs at their normal sites has improved. The band did not appear to shift by more than ~1/2 cm⁻¹ from 3569 cm⁻¹ in any of the TE specimens, heated or not, i.e., it always remains

cm ⁻¹	moiety
3800-3400	H ₂ O
3010	organic vapor (C-H on C = C or $\text{C} \equiv \text{C}$)
2960	organic vapor
2910, 2850	organic liquid (C-H) on cell windows
2400-2200	CO ₂
2000-1300	H ₂ O bending
1410, 1260	organic liquid
968, 932	organic vapor (C-H)

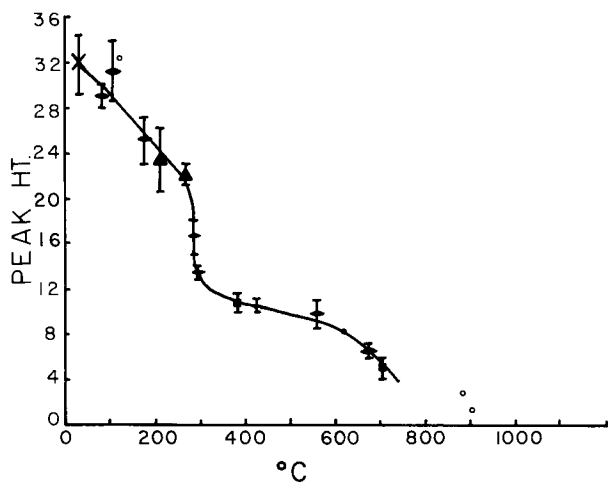


Fig. 4. Water remaining in TE specimen after it had been heated to indicated temperatures. Measurements were based on height-above-background of i.r. spectrum at 3300 cm^{-1} (see text). The number of data points contributing to each plotted point are: $\circ = 1$; $\diamond = 2$; $\blacktriangle = 3$; $\blacksquare = 4$; $\times = 5$

at least one wavenumber lower than the corresponding band in OHAp.

Further evidence of OH^- increase is given by the 3495 cm^{-1} band due to the OH -stretch motion perturbed from 3569 cm^{-1} by hydrogen bonding to a Cl^- neighbor substituting for an OH^- in the hexad-axis column [22]. Thereby Figure 7 shows again an increase in structural OH^- up to a maximum at $\sim 400^\circ\text{C}$.

Figures 6 and 7 show results for specimen heating runs made both in specially dried N_2 and in N_2 taken straight from the commercial supplier's tank with-

out special drying. Although the partial pressure of the water vapor accompanying the ordinary N_2 must be much less than that in air, it was sufficient for the TE specimens heated above $\sim 700^\circ\text{C}$ to remain hydroxylated or to rehydroxylate on cooling. This is shown by the relative absence of the OH^- bands in specimens heated above 700°C in the dried N_2 . We assume that the rehydroxylation is greater for the higher temperature because other things such as Cl^- and CO_3^{2-} (see next section) have been driven off and no longer take up possible OH^- sites. That the Cl^- has been largely driven off at the higher temperature is suggested by the fact that rehydroxylation affects the 3569 cm^{-1} band much more than the 3495 cm^{-1} band (Figs. 6 and 7 in the $600\text{--}1200^\circ\text{C}$ range). Other possible explanations, such as aggregating of the Cl^- or possible slow kinetics of re-establishing the hydrogen bonds, seem less likely; OH^- mobility is clearly high and the degree of hydroxylation is similar to the maximum degree of hydroxylation occurring near 400°C .

Carbonate and CO_2

The relative amount of B-site CO_3^{2-} indicated by the area (proportional to the apparent extinction coefficient) of the i.r. band at 1415 cm^{-1} is shown in Figure 8. Also shown is the amount of A-site CO_3^{2-} indicated by area of the 1546 cm^{-1} band and the amount of CO_2 indicated by the area of the 2340 cm^{-1} band. Note that the ordinates differ for the A-type and B-type CO_3^{2-} (and for CO_2); there is much more of the B-type present. Similar results were obtained with heating in N_2 and in the specially dried

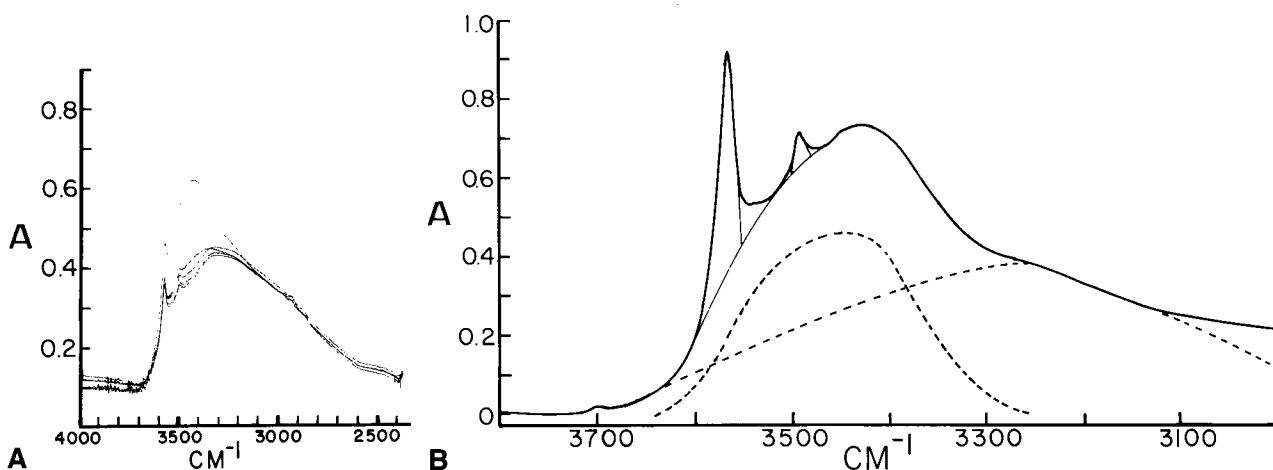


Fig. 5. The two contributions to the broad water band in i.r. spectra of TE A Repeated i.r. scans over $3600\text{--}3200\text{ cm}^{-1}$ region as the specimen in the KBr pellet became drier while in the i.r. unit in flowing dry N_2 . Note that only the higher wavenumber portion of the "band" is affected. Scan repeat rate was 2/h (A = absorption). B Visually estimated allocation of the composite band into two portions, partly on the basis of Fig. 5a

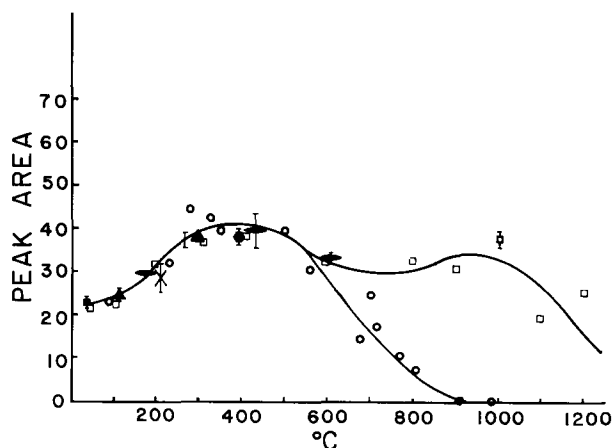


Fig. 6. Structural OH in TE at room temperature after being heated to the indicated temperatures, as determined from the 3569 cm^{-1} i.r. band (unperturbed OH stretch). Results for TE heated in N_2 straight from the tank are indicated by \square . Results for TE heated in specially dried N_2 are indicated by symbols which also identify the number of data points per plotted point, thus: $\circ = 1$; $\bullet = 2$; $\blacktriangle = 3$; $\blacksquare = 4$; $\times = 5$; $\bullet = 6$

N_2 . Unexpectedly, there is definite loss of B-CO_3^{2-} and probable loss of A-CO_3^{2-} even at 100°C . There is definite loss of A-type at 200°C . These results are quite at variance with the report of Davidson and Arends [18] that "the CO_3^{2-} bands remained practically constant" in the range $150^\circ\text{--}400^\circ\text{C}$. This variance may be due to different sample selection. Although they presumably heated for 24 h in N_2 at each temperature, much as we did, they used bovine enamel and only the outer $200\ \mu\text{m}$ (J. Arends, personal communication 1979).

A-CO_3^{2-} is generally agreed to be substituting for OH^- [e.g. 2, 23, 24], and what we now recognize as B-CO_3^{2-} is generally agreed to be substituting for PO_4^{3-} [15, 16, 25–29]. That places both types within the crystalline structure where, one would think, their mobility would be low. A check was made on the possibility that the initial losses might be of adsorbed CO_3^{2-} somehow having i.r. bands similar to A-CO_3^{2-} and B-CO_3^{2-} , rather than the much documented A and B species themselves. Evidence was sought of any shift in the band frequencies with increasing heating temperatures up to 400°C . None was found; the observational error was $<1\text{ cm}^{-1}$. Thus apparent decreases in both A and B CO_3^{2-} at temperatures $\leq 200^\circ\text{C}$ have to be accepted as probably real. It should be noted (see following discussion of CO_2) that most of the CO_3^{2-} lost at these low temperatures may remain in the crystal as CO_2 and, hence, the decrease would not be noted in wet chemical analyses such as Arends and Davidson used. Because of the low temperature, the mechanism of decrease should be sought in breakdown

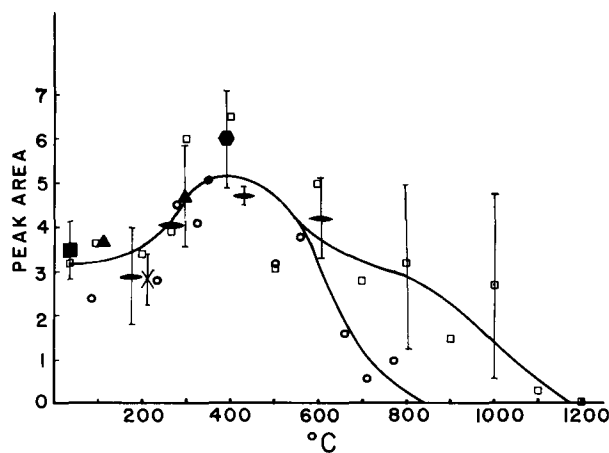


Fig. 7. Structural OH^- and Cl^- in TE, after heating, as determined from the 3495 cm^{-1} i.r. band (Cl^- -perturbed OH stretch). Symbols have the same meaning as in Fig. 6

rather than, necessarily, diffusion of the CO_3^{2-} completely out of the crystals. Further, the mechanism must account for the increase in A-CO_3^{2-} following the initial decrease. Two observations are relevant.

First, alternate heating of either hydroxyapatite or TE at 1000°C in a CO_2 stream and then H_2O vapor, or vice versa, causes a $2(\text{OH}^-) \leftrightarrow \text{CO}_3^{2-}$ exchange with the CO_3^{2-} going to A sites. The extent to which A-CO_3^{2-} builds up depends strongly on the dryness of the CO_2 stream, indicating that the chemical balance favors retention of OH^- instead of A-CO_3^{2-} when there is a substantial amount of A-CO_3^{2-} present [23, 30].

The second observation is the unexpected result (Fig. 8, i.r. band at 2340 cm^{-1}) that CO_2 is formed and partially retained in the specimen at a temperature of only $\sim 200^\circ\text{C}$. It is randomly oriented [15]. The following scenario now presents itself:

1. Even below 200°C , both A-CO_3^{2-} and B-CO_3^{2-} start to decompose with CO_2 the principal product, which then diffuses through and, no doubt, partially out of the crystallites.

2. If the B site is the PO_4^{3-} site, as is widely supposed, the CO_2 from breakdown of B-CO_3^{2-} is formed at a location adjoining the hexad axis channel (containing the A-CO_3^{2-} and OH^-), and the logical diffusion route for it out of the crystal is through the hexad axis channel.

3. As the decomposition proceeds more extensively at higher temperatures, the production rate of CO_2 exceeds the rate at which it can diffuse out and CO_2 (2340 cm^{-1}) builds up in the crystallite, in no specific crystallographic orientation. This lack of orientation suggests it is not in the hexad axis channels but, rather, probably still in the PO_4^{3-} site where it would be undersize for the site and hence

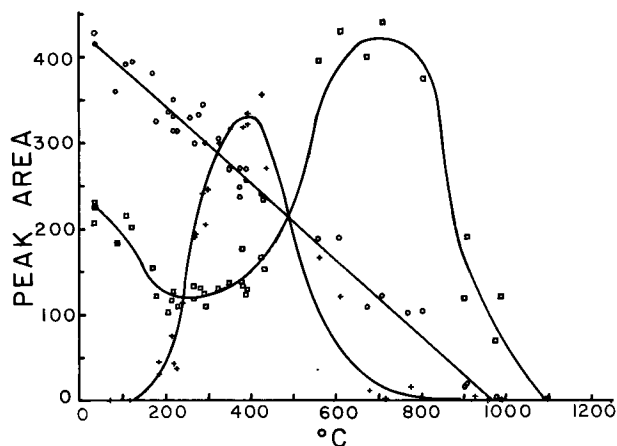


Fig. 8. CO_3^{2-} in TE, after heating, as determined from i.r. bands. Note that the ordinate values are relative only, and that the various species are actually plotted to different scales. \square , A-type, determined from area of 1546 cm^{-1} band. \circ , B-type, determined from area of 1415 cm^{-1} band. $+$, CO_2 , determined from area of 2340 cm^{-1} band

able to be in more than one orientation. The inferred absence of CO_2 , as such, in the hexad axis channel is consonant with the channel being an easy diffusion path and the ~ 24 h equilibration time at each temperature being long enough for the easy diffusion processes to become essentially completed.

4. The initial decrease in A-CO_3^{2-} (Fig. 8) correlates (qualitatively) with the increase in OH^- (Fig. 6), suggesting that the newly formed OH^- is displacing A-CO_3^{2-} in consonance with (a) the high temperature observation of the dominance of OH^- over A-CO_3^{2-} if the OH^- is available [23] and (b) the small added mobility, arising from the increased temperature, to make the reaction "go." The predicted reaction is $\text{H}_2\text{O} + \text{CO}_3^{2-} \rightarrow 2(\text{OH})^{1-} + \text{CO}_2$, with the H_2O coming from that already in TE [1, 6] and inferred here (see section on lattice parameters) to be in the hexad axis channels.

5. At temperatures near 400°C , increased mobility of the CO_2 formed from B-CO_3^{2-} brings more of it into the channels. At the same time, OH^- stops increasing and soon starts to decrease. Thus the supply of CO_2 and the removal of OH^- favor the formation of A-CO_3^{2-} , which then increases.

6. With less CO_2 being supplied to the hexad axis channels, the build-up of A-CO_3^{2-} stops as decomposition rate exceeds formation rate.

7. Finally, at the highest temperatures, e.g., 1100°C , all CO_3^{2-} and CO_2 have been driven off, OH^- and Cl^- are gone, and the principal crystalline phase [some $\beta\text{-Ca}_3(\text{PO}_4)_2$ occurs as a minor second phase] is probably essentially an oxyapatite if rehydroxylation is prevented on cooling [2, 23, 31, 32].

We conclude, then, that the B-CO_3^{2-} in TE does partially transform to A-CO_3^{2-} , but that it probably does so through the intermediate of CO_2 . The possibility that CO_3^{2-} migrates as such to the hexad axis channel where it would then be A-CO_3^{2-} , without the need for a CO_2 intermediate, is not excluded but is thought to be unlikely just on electrostatic grounds.

Let us return to the lower temperature and ask if the reaction $\text{CO}_3^{2-} + \text{H}_2\text{O} \rightarrow 2(\text{OH})^- + \text{CO}_2$ is capable of explaining quantitatively the initial decrease of A-CO_3 and concomitant increase in OH^- . We ignore for this calculation the possibility that structural H_2O may not be the only source of OH^- (3569 cm^{-1}). (Note in Fig. 3, for example, that organic species are being evolved at 250°C , presumably releasing H_2O and possibly OH^- in the process. In fact, from the Dowker and Elliott work [15], it seems that decomposition of the organic fraction produces the N-C-O moiety giving rise to the 2200 cm^{-1} i.r. band.) Working only with the data from 25° to 220°C , one finds $\sim 40\%$ decrease in A-CO_3^{2-} (Fig. 8.) and $\sim 40\%$ increase in OH^- (Fig. 6). Let the maximum OH^- ever present correspond to an at least 80% hydroxylated apatite. Then the amount initially present, which is $\sim 54\%$ of the maximum, is about $0.54 \times 1.6 = 0.86$ OH^- ions per unit cell. The increase up to 220°C is, then, $0.3 \times 0.86 = 0.26$, or ~ 1 OH^- per four unit cells.

The amount of A-CO_3 required to provide this, by the reaction stated, is ~ 0.13 A-CO_3^{2-} per cell. Since this is to be 40% of the amount initially present, then the initial amount of A-CO_3^{2-} required to account for all OH^- increase would be ~ 0.33 A-CO_3 per cell, or ~ 2 wt%. Although there is ~ 3 wt% CO_3 present in TE, Elliott [2], for example, has estimated that no more than 15% of it is in the A sites. A direct test of the amount of a nearly fully carbonated synthetic A-type carbonate apatite required in the reference i.r. beam to compensate the A-CO_3^{2-} bands in TE indicated ~ 1 wt% A-CO_3^{2-} in TE (i.e., one A-CO_3^{2-} per 6 cells). Thus, at most, only one-half of the increase in OH^- (between 25° and 220°C) can be ascribed to the $\text{H}_2\text{O} + \text{CO}_3^{2-}$ reaction. On the other hand, all of the decrease in A-CO_3^{2-} can be readily accounted for by this mechanism.

HPO₄²⁻ and Pyrophosphate

An i.r. band at 875 cm^{-1} was used by Montel et al. [33] to follow changes in HPO_4^{2-} content in some synthetic nonstoichiometric "apatites" and implied a correspondence between the HPO_4^{2-} so indicated and the pyrophosphate found on heating (the Gee and Deitz [34] method for determining HPO_4^{2-} content). Unfortunately, there are also two CO_3^{2-}

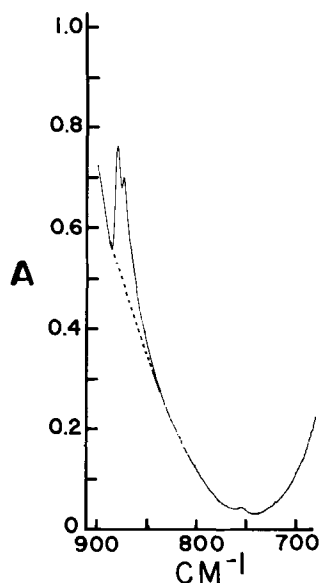


Fig. 9. i.r. doublet at 872 cm^{-1} and 879 cm^{-1} in TE after heating to 700°C. This example is typical of the resolution consistently obtained in this work. Machine reproducibility is evidenced by the fact that 3 scans are shown. The dashed line shows the systematically drawn "background" line above which the heights of the two peaks were measured

bands in this region. Arends and Davidson [3] reported measuring the HPO_4^{2-} present in bovine tooth enamel by separating out the contributions of HPO_4^{2-} and CO_3^{2-} to the unresolved (in their case) i.r. doublet centered at $\sim 875 \text{ cm}^{-1}$. Elliott [2, 35] had reported this composite band to be a doublet at 872 cm^{-1} and 879 cm^{-1} ascribed to CO_3^{2-} in two different sites. In the present work the doublet was consistently resolved (Fig. 9) and the temperature dependences of the two parts, at 872 and 879 cm^{-1} , were followed separately (Fig. 10) in the hope of monitoring the thermal decomposition of HPO_4^{2-} through its contribution to one or both of these bands.

Another possible parallel monitor of HPO_4^{2-} decomposition would be pyrophosphate formation [34]. Herman and Dallemagne [36] showed with wet chemistry that the pyrophosphate content of TE was maximized at $\sim 600^\circ\text{C}$, as did Berry [37] in synthetic hydroxyapatite. Unfortunately, the i.r. bands for the β form at 725 cm^{-1} [38] and for the γ form at 715 cm^{-1} [37, 39] were too weak to provide useful monitoring of the development of pyrophosphate. Rather qualitative assays were made with X-ray diffraction patterns of TE samples heated 24 h in dry N_2 at 400°C, 600°C, and 800°C, respectively. Much as would be expected, essentially no pyrophosphate ($\text{Ca}_2\text{P}_2\text{O}_7$) was present in the 400°C specimen, both $\gamma\text{-Ca}_2\text{P}_2\text{O}_7$ and $\beta\text{-Ca}_2\text{P}_2\text{O}_7$ (roughly 2 wt% of the β form) were in the 600°C one, and the β form with little or none of the γ form in the 800°C specimen.

Therefore, one should expect whatever contribution HPO_4^{2-} makes to the i.r. bands at 872 and 879 cm^{-1} to decrease markedly in the range starting below 600°C. However, in the range 500–800°C both of these bands increase in intensity (Fig. 11). Thus the change in neither band can be simply ascribed to HPO_4^{2-} ; the changing CO_3^{2-} contributions must also be taken into account. The increase in the 879 cm^{-1} band does correlate qualitatively with the increase of A- CO_3^{2-} as indicated by the 1546 cm^{-1} band (Fig. 8). Thus we ascribe it to A- CO_3^{2-} , leaving the 872 cm^{-1} band for B- CO_3^{2-} in TE, in accord with Elliott [2].

Arends and Davidson [3] report a $> 30\%$ decrease in the combined doublet extinction coefficient (averaged at 875 cm^{-1}) after 400°C heating, which agrees well with the results in Figure 10. At higher temperatures, however, the agreement fails.

Up to $\sim 400^\circ$ the 872 cm^{-1} band behavior correlates well with that of the 1415 cm^{-1} band (Fig. 8), as it should if both represent B- CO_3^{2-} . But thereafter the 872 cm^{-1} band increases, whereas the 1415 cm^{-1} band continuously decreases. Presumably, such a difference could be caused by changing environment of the CO_3^{2-} causing the relative oscillator strengths of the two modes (1415 and 872) to change, but that is considered to be unlikely as there are no shifts in position even as small as two wavenumbers. Further, we know that the B- CO_3^{2-} (and CO_2) does leave the specimen. Thus something else, which increases with temperature, is contributing to the measured height of the 872 cm^{-1} peak above 400°C. Perhaps this can be ascribed in part to the tail of the 879 cm^{-1} peak, which does increase strongly in this temperature range. More interestingly, Montel and Heughebaert [40] have reported that in synthetic preparations the presence of F inhibits the decrease, on heating to 600°, of the "875 cm^{-1} band" because of the high temperature formation of PO_3F^{2-} ions which, they suggest, have an i.r. band at the same frequency.

The 879 cm^{-1} band follows the 1546 cm^{-1} band (A- CO_3^{2-}) qualitatively very well. Quantitatively, however, it has not increased proportionately above 600°C. Might that be due to loss of HPO_4^{2-} contributing at the 879 cm^{-1} frequency? Assuming that both the 1546 cm^{-1} and the 879 cm^{-1} bands represent only A- CO_3^{2-} at 600 and 700°C, one can calculate what the 879 cm^{-1} band intensity would be at the lower temperatures if it followed the trend of the 1546 cm^{-1} band. This procedure was carried out for 100° intervals with the solid line curves—not the individual data points—shown in Figures 8 and 10 for the bands in question. No point at 800°C was included because of uncertainties in the rapidly changing curve shapes and heights there. On the as-

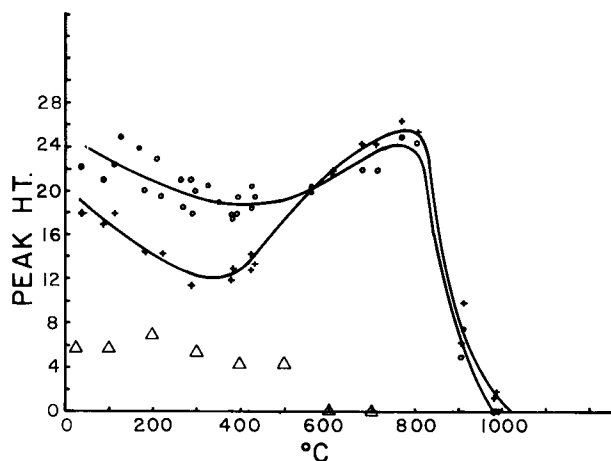


Fig. 10. Band height measures derived from 872–879 cm^{-1} doublet. ○, 872 cm^{-1} (B-CO_3^{2-}), +, 879 cm^{-1} (A-CO_3^{2-} and, possibly, HPO_4^{2-}). Δ, Portion of 879 cm^{-1} band height that is possibly assignable to HPO_4^{2-}

assumptions that (a) the HPO_4^{2-} band is at 879 cm^{-1} (no evidence of change in the 879 cm^{-1} band width in the range 400–800°C was found) and (b) the ratio of band width to peak height is not changing, the difference between the two curves for the 879 cm^{-1} (Fig. 10) band could be ascribed to the otherwise unobserved HPO_4^{2-} . In favor of this assignment is the fact that this difference curve goes to zero in the temperature range (500–600°C) where pyrophosphate appears.

There is no evidence for HPO_4^{2-} in TE to be transformed below 400°C, and what evidence there is suggests that the transformation (to pyrophosphate) takes place above 500°C, in agreement with Ciesla, Maciejewski, and Rudnicki [41].

Species of Organic Origin

An i.r. band at 2200 cm^{-1} , initially thought to be oriented CO_2 , has now been shown by Dowker and Elliott [15] to be due to the ion $(\text{NCO})^{1-}$ produced from residual nitrogenous species associated with synthetic apatite preparations formed in solutions containing ammonium ions. In TE, they ascribe its origin to the breakdown of the organic component. In that case, the temperature dependence of this 2200 cm^{-1} band is an indicator of the progress of the breakdown of the organic component of TE. This band starts developing at ~400°C, is at a maximum at about 600°C, and disappears only above 750–800°C. This fact suggests that the organic component is not fully decomposed at 600°C (in the essentially O_2 -free atmosphere for times used). This observation correlates with the fact that TE heated

at 600°C (in an earlier experiment for other purposes) was gray whereas that heated at 1,000°C was white.

A band at 756 cm^{-1} shows much the same temperature dependence as does the 2200 cm^{-1} band. Rowles [42] reported $\alpha\text{-Ca}_2\text{P}_2\text{O}_7$, and the absence of the β and γ forms, in a nonstoichiometric apatite heated at 650°C for 18 h. B.O. Fowler (personal communication) has identified a P-O-P i.r. band in $\alpha\text{-Ca}_2\text{P}_2\text{O}_7$ at 755 cm^{-1} . However, X-ray diffraction showed β and γ forms but no $\alpha\text{-Ca}_2\text{P}_2\text{O}_7$ present. Thus the 756 cm^{-1} band remains unidentified with the suggestion that, like the 2200 cm^{-1} band, it may be of organic origin.

Lattice Parameter

The a lattice parameter values are shown in Figure 11. The principal new results for a are that (a) the temperature at which the contraction occurs has been better defined; (b) the thermal coefficient of expansion is greater before the contraction and its temperature dependence indicates increasing disorder as the contraction temperature is approached; (c) the contraction temperature is between 250° and 300°C and is somewhat affected by kinetics; (d) the actual a contraction in this region is ~0.014 Å; (e) the TE specimen must be heated to temperatures high enough to drive off all CO_3^{2-} , e.g., 1000°C, before the full 0.023 Å contraction to the hydroxyapatite value can be observed (Table 1); and (f) the mechanism of the further expansion, following the initial contraction, is here recognized as the production and retention of additional CO_3^{2-} in A sites. The effect is at a maximum at ~800°C, for which temperature LeGeros et al. [4] had noted the fact of expansion.

The cause of the sharp contraction of a between 200° and 300°C can not be a sudden loss of HPO_4^{2-} . The analysis in the preceding section shows that whatever HPO_4^{2-} conversion there is in TE occurs at a much higher temperature, i.e., in excess of 400°C. Neither can the a contraction be due to loss of Cl^- , both because too little is initially present (~0.3 wt%) to account for it all (from $a = 9.65$ Å for chlorapatite, $a = 9.42$ Å for hydroxyapatite, and Vegard's law, the expected effect of 0.3 wt% Cl^- substituting for OH^- is to increase a by ~0.009 Å) and, more importantly, because the evidence is that no Cl^- is lost up to that temperature (Fig. 6). Corcia and Moody [7], by mass spectrometry, also did not observe any Cl^- loss up to 1000°C. In fact, the TGA and difference-TGA curves, including that of Davidson and Arends [18] shown in the Figure 2, inset, show minimal weight loss in the 200–250°C range.

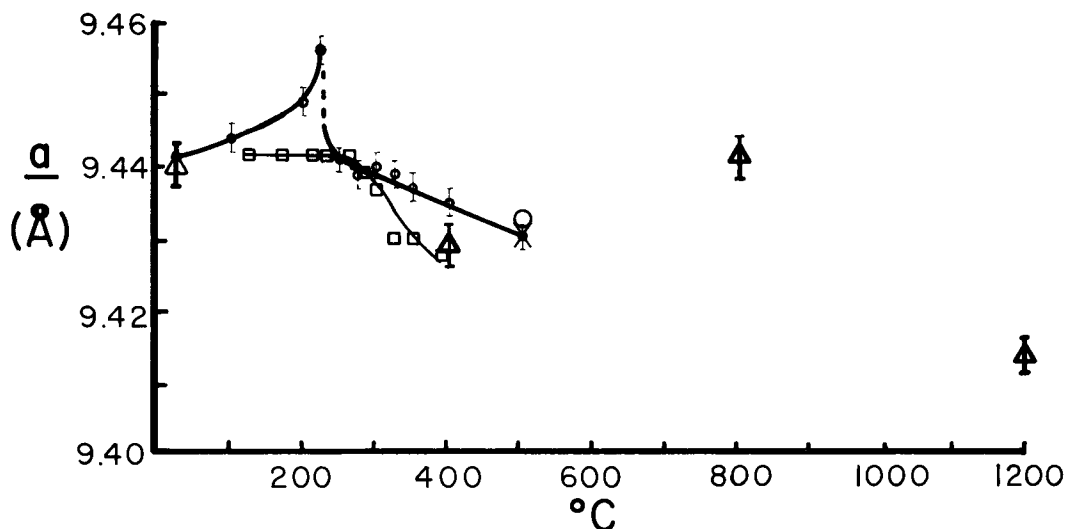


Fig. 11. a lattice parameters. \circ , a calculated for room temperature from measurements made in vacuum at indicated temperature and "corrected" to room temperature with the thermal expansion factor $\alpha(a) = 1.02 \times 10^{-6} \text{ \AA}/^\circ\text{C}$ observed in 2nd and subsequent heating cycles. \times , \circ , a measured at 25°C after 1st and 2nd 500°C heating cycles in vacuum. \triangle , a measured at 25°C after TE was heated in N_2 . For this and the above two sets of a results, the lattice parameters were determined as an incidental part of complete Rietveld analyses of entire powder X-ray diffraction patterns. \square , a determined from shift of 3.00 X-ray Bragg reflection relative to its position in untreated TE (for which a was taken to be 9.4415 Å) Heating was done in N_2 atmosphere and the X-ray measurements were made at room temperature

For specimens heated for several hours in N_2 , the main contraction does, however, coincide within 10–15°C with the "sudden" loss of structural H_2O (3300 cm^{-1}) (see Figs. 11 and 4). It seems reasonable to conclude that the structural H_2O is associated with the enlarged (cf. OHAp) a axis of TE. The dramatic changes in both occur in the range 270–300°C. The lattice parameters measured in vacuum appear to contract at lower temperatures, e.g., 230–240°C, which is consistent with a kinetically limited effect appearing at higher temperatures when the specimen is heated for shorter times (hours in N_2 at atmospheric pressure vs days in vacuum). The TGA curve shows nothing dramatic happening at 250–300°C but, rather, at 325–400°C. Since the TGA is a dynamic heating experiment, it may well be that that actual specimen temperature is lower than indicated. Further, in the TGA experiment there is little or no chance for slow diffusion to occur so, again, the observed temperature for large change would be displaced upward by kinetic limitations. Thus we must regard the TGA curve as corroborating, more than contradicting, the H_2O and Δa results.

It is proposed that the sharp contraction in a is accompanied by a reordering phenomenon. There are several bits of circumstantial evidence for this: (a) The decomposition of both A- CO_3^{2-} and B- CO_3^{2-} plus, especially, the appearance of CO_2 in the region below 250°C show that the atomic thermal vibrations of the apatite atoms have become suf-

ficient for some atomic rearrangement (CO_3^{2-} breakdown) and molecular mobility to occur. (b) The increase in structural OH^- (Fig. 4) demonstrates that there is some activity in the hexad axis channel region which entails either reordering or transport, or both. (c) The increasing expansion rate of a (in vacuum) prior to its contraction signifies some activity within the lattice, such as thermal vibrationally caused expansion of disordered regions prior to their crossing a mobility threshold (i.e., sufficient kinetic energy) which permits their components to rearrange into an ordered, lower free energy, smaller volume configuration.

We conclude that the actual $\sim 0.014 \text{ \AA}$ contraction of a in the 250–300°C region is associated with a loss of structural ("incorporated") H_2O , much as LeGeros, Bonel, and LeGros [6] suggested, and is accompanied by "sudden" (in temperature) reordering made possible by the increased thermal vibrations of both the affected ions and

Table 1. TE Lattice Parameters After Heating

Heating Temperature (°C)	Lattice parameters at 25°C	
	a (Å)	c (Å)
Room temp.	9.440 (6)	6.872 (4)
400	9.428 (3)	6.880 (2)
800	9.441 (3)	6.875 (2)
1200	9.414 (2)	6.885 (1)

their constraining lattice structure, plus any vacancies created by the cumulative losses of CO_3^{2-} and H_2O up to this point. The situation may be viewed rather like a key turning in a lock; the various forces toward change build up gradually with temperature until a point is reached at which the lock bolt suddenly starts to move on its own and quickly falls into place in the final position. We further conclude, then, that a of TE is $\sim 0.023 \text{ \AA}$ larger than that of hydroxyapatite ($a = 9.421 \text{ \AA}$) both because of disorder in some of the constituents and because of the presence of structural H_2O . The disorder seems a reasonable expectation for materials formed at temperatures so low (37°C) that atom and ion mobility within the precipitated solid would be too low for the minimum free-energy configuration to be reached. Other evidence for disorder in the hexad axis region of TE has been reported by Young and Holcomb [43], who found that TE deuterizes much more readily than does hydroxyapatite that has been heated above 450°C .

It is relevant to note that LeGeros [5] has observed a similar a axis contraction, after 400°C heating, in all synthetic apatites prepared from aqueous systems. It would appear that the same arguments should apply and would lead to the same mechanism for these aqueous preparations.

Turning now to the increase in a (measured at 25°C) with heating temperatures, one sees that the expansion of the a axis in the $600\text{--}800^\circ$ region correlates with the build-up of A-CO_3^{2-} . A-site CO_3^{2-} expands a by $\sim 0.024 \text{ \AA/wt\% CO}_3^{2-}$ in hydroxyapatite partially converted to A-type carbonate apatite at high temperatures ($a = 9.54 \text{ \AA}$ for $\sim 85\%$ carbonation [2, 23]). Table 1 shows the lattice parameter results for a particular set of samples. When the 1200° result is used as the base (because all H_2O and CO_3^{2-} are driven off by that heating), the a axis expansion in the 800° specimen is, nominally, 0.027 \AA . In the 800° specimen there is left about 20% of the initial B-CO_3^{2-} (Fig. 8), and this should have the effect of decreasing the a axis at the rate of $0.01 \text{ \AA per } 1.7 \text{ wt\% CO}_3^{2-}$ (Fig. 9 of reference 25). Taking the amount of CO_3^{2-} initially present to be 2.8 wt% (Arends and Davidson [3] report 2.8(5) wt% average for 10 experiments) and 90% of it in B sites (14), one calculates $0.20 \times 0.90 \times 2.8 \text{ wt\%} = 0.50 \text{ wt\% B-CO}_3^{2-}$ nominally left after heating to 800°C . Its effect on the a parameter, then, should be to contract it by $(0.01 \text{ \AA}/1.7 \text{ wt\%}) 0.50 \text{ wt\%} = 0.003 \text{ \AA}$. Thus the total a expansion in the 800°C specimen to be accounted for is, nominally, $0.027 + 0.003 = 0.030 \text{ \AA}$. If this were due entirely to A-CO_3^{2-} , it would imply $\sim 1.25 \text{ wt\%}$ present, or that $\sim 20\%$ of the possible A-CO_3^{2-} sites are filled. The probable error in this estimate arising just from the reported

errors in CO_3^{2-} content and a values is $\sim 40\%$ of the 20%. Thus our estimate of the number of A-CO_3^{2-} sites filled is more informatively stated as 12–28%. From comparison of the i.r. band intensity with those observed in other work (unpublished) in this laboratory on high-temperature carbonate apatites of known A-CO_3^{2-} content, an estimate of 10–13% A-site filling was obtained. In view of the probable errors involved, these two estimates are in satisfactory agreement. We conclude, then, that (a) the expansion of the a axis of TE caused by heating in the range $600\text{--}800^\circ\text{C}$ is primarily due to the presence of A-CO_3^{2-} formed from B-CO_3^{2-} via CO_2 intermediaries and (b) the amount of A-CO_3^{2-} present after 800° heating is substantial, filling more than 10% of the possible A sites.

The fraction of the initially present B-CO_3^{2-} that is processed to A-CO_3^{2-} also must be substantial. According to the above estimates $\sim 1 \text{ wt\%}$ (0.6–1.8 wt%) of A-CO_3^{2-} still remains when the 800° specimen is cooled to room temperature. This is $1/4$ to $1/3$ of the amount of B-CO_3^{2-} initially present. Considering that A-CO_3^{2-} must be being lost all along the way (since it is lost at temperatures below 200°C , see Fig. 7), it seems probable that most of the B-CO_3^{2-} must go through an A-CO_3^{2-} stage in the process of getting out of the apatitic crystals of TE.

Does this mean that some exchange between B-CO_3^{2-} and A-CO_3^{2-} can be expected *in vivo*? Although it is doubtful that it would occur at any great rate, because of the kinetics, it would seem to be possible at very low rates.

Acknowledgements. We thank Dr. J.C. Elliott for discussions and a early draft copy of Dowker and Elliott [15] work. Dr. P.E. Mackie for the a lattice parameter determinations in vacuum at temperature, B.O. Fowler for many helpful comments on the manuscript, and the National Institutes of Health for financial support under NIDR Grant DE-01912.

References

1. Little, M.F., Casciani, F.S.: The nature of water in sound human enamel. A preliminary study. *Arch Oral Biol* **11**:565–571, 1966
2. Elliott, J.C.: The crystallographic structure of dental enamel and related apatites. Ph.D. Thesis, University of London, 1964
3. Arends, J., Davidson, C.L.: HPO_4^{2-} content in enamel and artificial carious lesions. *Calcif Tissue Res* **18**:65–79, 1975
4. LeGeros, R.Z., Trautz, O.R., LeGeros, J.P., Klein, E.: Pyrolysis of biological apatites: X-ray diffraction and infrared studies, 48th General Assembly of the International Association of Dental Research, 16–19 March 1970, New York, NY Abstract #177
5. LeGeros, R.Z.: The unit-cell dimensions of human enamel apatite: effect of chloride incorporation. *Arch. Oral Biol.* **20**:63–71, 1974
6. LeGeros R.Z., Bonel, G., Legros, R.: Types of " H_2O " in human enamel and precipitated apatites. *Calcif. Tissue Res.*

- 26:111-118, 1978
7. Corcia, J.T., Moody, W.E.: Thermal analysis of human dental enamel, *J. Dent. Res.* **53**:571-579, 1974
 8. Myrberg, N.: Proton magnetic resonance in human dental enamel and dentine, *Trans. R. Schs. Dent. Stockh Umea*, No. 14, 3-62, 1968
 9. Myers, H.M.: Trapped water in dental enamel, *Nature* **206**:713-714, 1965
 10. Holager, J.: Thermogravimetric examination of enamel and dentin, *J. Dent. Res.* **49**:546-548, 1970
 11. Brauer, G.M., Termini, D.J., Burns, C.L.: Characterization of components of dental materials and components of tooth structure by differential thermal analysis, *J. Dent. Res.* **49**:100-110, 1970
 12. Emerson, W.H., Fischer, E.E.: The infra-red absorption spectra of carbonate in calcified tissues, *Arch. Oral Biol.* **7**:671-683, 1962
 13. Bonel, G., Montel, G.: Etude comparee des apatites carbonates obtenues par differentes methodes de synthese, *Reactivity of Solids, 5th International Symposium Munich 1964*. Elsevier Publishing Co., Amsterdam, 1965
 14. Elliott, J.C.: On the interpretation of the carbonate bands in the infra-red spectrum of dental enamel, *J. Dent. Res.* **42**:1081, 1963
 15. Dowker, S.E.P., Elliott, J.C.: Infra-red absorption bands from NCO^- and NCN^{2-} in heated carbonate-containing apatites prepared in the presence of NH_4^+ ions, *Calcif. Tissue Int.* **29**:177-178, 1979
 16. LeGeros, R.Z.: Effect of carbonate on the lattice parameters of apatite, *Nature* **206**:403-404, 1965
 17. Termine, J.D., Lundy, D.R.: Hydroxide and carbonate in rat bone mineral and its synthetic analogs, *Calcif. Tissue Res.* **13**:73-83, 1973
 18. Davidson, C.L., Arends, J.: Thermal analysis studies on sound and artificially decalcified tooth enamel, *Caries Res.* **11**:313-320, 1977
 19. Young, R.A., Mackie, P.E., von Dreele, R.B.: Application of the pattern-fitting structure-refinement method to X-ray powder diffractometer patterns, *J Appl. Cryst.* **10**:262-269, 1977
 20. Aoki, H., Ban, T., Akao, M., Kato, K., Iwai, S: Thermal analysis of calcified tissues, *Rep. Inst. Med. Dent. Eng. (Tokyo)* **11**:25-31, 1977
 21. Bartlett, M.L., Young, R.A.: Structural OH deficiency in tooth enamel and hydroxyapatite, *Program and Abstracts of 55th General Session of the International Association for Dental Research*, 23-26 March 1972, Las Vegas, Nevada, Abstract #125
 22. Dykes, E., Elliott, J.C.: The occurrence of chloride ions in the apatite lattice of Holly Springs hydroxyapatite and dental enamel, *Calcif. Tissue Res.* **7**:241-248, 1971
 23. Bonel, G.: Contribution a l'etude de la carbonation des apatites. Thèse, L'Université de Paul Sabatier de Toulouse, France, 1970
 24. Bonel, G., Montel, G.: Sur une nouvelle apatite carbonatée synthétique, *C.R. Acad. Sci [D] (Paris)* **258**:923-926, 1964
 25. LeGeros, R.Z., Trautz, O.R., LeGeros, J.P., Klein, E.: Carbonate substitution in the apatite structure, *Bull. Soc. Chim. France (n° special)* 1712-1718, 1968
 26. Borneman-Starinkevitch, I.D.: On isomorphic substitutions in carbonate apatite, *Dokl. Acad. Nauk SSR* **22**:113-115, 1939
 27. McConnell, D.: The problem of the carbonate apatites. IV. Structural substitutions involving CO_3 and OH, *Bull. Soc. Fr. Mineral. Crist.* **75**:428-445, 1952
 28. Trautz, O.R.: Crystallographic studies of calcium carbonate phosphate, *Ann. N.Y. Acad. Sci.* **85**:145-160, 1960
 29. Hendricks, S.B., Hill, W.L.: The inorganic constitution of bone, *Science* **97**:255-257, 1942
 30. Young, R.A., Bartlett, M.L., Spooner, S., Mackie, P.E., Bonel, G.: Reversible high temperature exchange of carbonate and hydroxyl ions in tooth enamel and synthetic hydroxyapatite, *J. Biol. Physics (in press)*
 31. Trombe, J.C., Montel, G.: Sur l'oxyapatite phosphocalcique, *C.R. Acad. Sci. [D] (Paris)* **274**:1169-1172, 1972
 32. Trombe, J.C., Montel, G.: Some features of the incorporation of oxygen in different oxidation states in the apatitic lattice. I. On the existence of calcium and strontium oxyapatites, *J. Inorg. Nucl. Chem.* **40**:15-21, 1978
 33. Montel, G., Bonel, G., Trombe, J.C., Heughebaert, J.C., Rey, C.: Relations entre la physico-chimie des apatites et leur comportement dans les milieux biologiques et les différents traitements industriels, *Proceedings, First International Congress on Phosphorus Compounds, 17-21 October 1977*, 321-346, Rabat, Maroc, L'Institut Mondial du Phosphate, Paris, 1977
 34. Gee, A., Deitz, V.R.: Pyrophosphate formation upon ignition of precipitated basic calcium phosphate, *J. Am. Chem. Soc.* **77**:2961-2965, 1955
 35. Elliott, J.C.: The interpretation of the infra-red absorption spectra of some carbonate-containing apatites. In M.V. Stack, R.W. Fearnhead (eds.): *Tooth Enamel, its Composition, Properties and Fundamental Structure*. John Wright & Sons, Ltd., Bristol, 1965
 36. Herman, H., Dallemagne, M.J.: The main mineral constituent of bone and teeth, *Arch. Oral Biol.* **5**:137-144, 1961
 37. Berry, E.E.: The structure and composition of some calcium deficient apatites, *J. Inorg. Nucl. Chem.* **29**:317-327, 1967
 38. Fowler, B.O., Moreno, E.C., Brown, W.E.: Infra-red spectra of hydroxyapatite, octacalcium phosphate and pyrolysed octacalcium phosphate, *Arch. Oral Biol.* **11**:477-492, 1966
 39. Cant, N.W., Bett, J.A.S., Wilson, G.R., Hall, K.W.: The vibrational spectrum of hydroxyl groups in hydroxyapatite, *Spectrochim. Acta* **27A**:425-439, 1971
 40. Montel, G., Heughebaert, J.C.: Influence of fluoride on calcium orthophosphates hydrolysis, *Fluoride and Bone Symposium 2nd CEMO*, 9-12 Oct 1977, 82-93
 41. Ciesla, K., Maciejewski, M., Rudnicki, R.: Thermal decomposition of calcium hydroxyapatite and solid-state reactions with calcium fluoride and dicalcium pyrophosphate, *Proc. Nauk. Akad. Ekon. im. Oskara Langego Wroclawiu* **132**:301-303, 1978
 42. Rowles, S.L.: Discussion of first session. in M.V. Stack, R.W. Fearnhead (eds.): *Tooth Enamel its Composition, Properties, and Fundamental Structure*, p. 57. John Wright & Sons, Ltd., Bristol, 1965
 43. Young R.A., Holcomb, D.W.: Hydroxyapatite variability shown by deuteration, *J. Dent. Res.* **55**:B255, 1976

Received September 24, 1979 / Revised December 9, 1979 / Accepted January 9, 1980